Available online at www.sciencedirect.com
SCIENCE DIRECT
Polymer 47 (2006) 5364–5370
polymer
www.elsevier.com/locate/polymer

Solubility and diffusivity of solvents by packed column inverse gas chromatography

James V. Scicolone [a], Peter K. Davis [b], Ronald P. Danner [a,*], J. Larry Duda [a]

[a] *Department of Chemical Engineering, Center for the Study of Polymer–Solvent Systems, The Pennsylvania State University, University Park, PA 16802, USA*
[b] *GE Global Research, One Research Circle, Niskayuna, NY 12309, USA*

Received 31 March 2006; received in revised form 12 May 2006; accepted 15 May 2006
Available online 12 June 2006

Abstract

Inverse gas chromatography was used with solid polymer particles in packed columns to measure polymer–solvent solubility and diffusion. A new model for this IGC technique has been developed and used to obtain experimental results for *n*-pentane, isopentane, 1-hexene, *n*-hexane, and 1-octene solvents in polymer beads of polyethylene. The conditions were measured for solvents at infinite dilution, and experimental data were obtained for the binary polymer–solvent systems in a temperature range from 70 to 100 °C.

Keywords: Inverse gas chromatography; Solubility; Diffusivity

1. Introduction

In many polymerization processes chemical reaction of the monomer occurs in a fluidized bed of catalyst and monomer. As polymerization proceeds, small pellets of polymer particles are formed and, after the reaction terminates, the residual monomer must be removed from these pellets. This is usually accomplished by devolatilizing the pellets in large purge towers. The fundamental mechanisms behind the impurity separation are complex, and proper design of purge towers requires fundamental properties of the polymer–solvent system. Of key importance are the diffusion coefficient and the solubility of the solvent in the polymer pellets.

Inverse gas chromatography (IGC) has long been used to study sorption and diffusion in polymer–solvent systems [1–12]. IGC is a technique used to study the properties of a polymeric stationary phase by passing a pulse of solvent through a column filled with the stationary phase. The polymeric stationary phase is usually put into the column by one of two techniques. In the first technique, a thin polymer film is cast onto inert support particles. These coated particles are then packed into the column. This is commonly referred to as packed column IGC (PCIGC). A problem with PCIGC is that the coating thickness is non-uniform, making diffusion coefficient measurements difficult [6]. In the second technique, the polymer is cast as a thin film on the inside of a capillary wall. This technique is referred to a capillary column IGC (CCIGC). The advantage of CCIGC is that very uniform polymer coatings can be obtained.

In this work, a variation of the PCIGC technique is presented where solid polymer particles were packed into the column rather than coating on inert support particles. Although the surface of the solid polymer pellets is not very uniform, the surface non-uniformity is usually very small compared to the overall size of the pellet. This type of approach has been taken by Gray and Guillet [4] and Braun and Guillet [13]. An advantage this technique has over typical IGC methods is that experiments can be conducted on the actual particles from a reactor. Usually, the effluent pellets from a reactor need to be devolatilized of residual monomer and solvent. While most techniques to measure diffusion and partition coefficients destroy the morphology and porosity of the sample by compression into a film or dissolution in a solvent, this PCIGC technique allows measurements of effective diffusion and partition coefficients to be made on the unchanged pellets. Another advantage this technique has over solvent casting type IGC techniques is that some polymers are quite difficult to dissolve in a solvent. Such polymers could easily be studied with this PCIGC technique.

To obtain diffusion and partition coefficients from experimental elution profiles, a theoretical model was developed similar to that of Marcis [8] for CCIGC. The model accounts

* Corresponding author. Tel.: +1 814 8634814; fax: +1 814 8657846.
E-mail address: rpd@psu.edu (R.P. Danner).

0032-3861/$ - see front matter © 2006 Elsevier Ltd. All rights reserved.
doi:10.1016/j.polymer.2006.05.047

Nomenclature

ρ	mass concentration of solvent in the polymer phase (g/cm^3)	r'	r/τ
C	mass concentration of solvent in the vapor phase (g/cm^3)	R	ideal gas constant
C_0	strength of the solvent pulse ($g\ s/cm^3$)	t	time (s)
D_p	diffusion coefficient in the polymer phase (cm^2/s)	t'	tV/L
D^{eff}	effective diffusion coefficient in the polymer phase (cm^2/s)	V	carrier gas velocity (cm/s)
E^{eff}	effective activation energy of diffusion	z	axial coordinate (cm)
ΔH^{eff}	effective heat of absorption	*Greek symbols*	
K_p	partition coefficient (concentration in polymer phase/concentration in vapor phase)	α	$\chi/[K_p(1-\chi)]$
K_s	surface adsorption equilibrium constant	β	$\sqrt{V\tau^2/LD_p}$
L	column length (cm)	γ	D_g^{eff}/VL
r	radial coordinate (cm)	ε	$3K_s(1-\chi)/\tau\chi$
		χ	void fraction in column
		ρ'	$\rho L/K_p C_0 V$
		τ	polymer bead radius

for both bulk absorption/diffusion and surface adsorption and was solved using a Laplace transform technique.

2. Theoretical development

In the PCIGC experiments conducted in this study, a column was packed with solid polymer particles. In the following derivations, it is assumed that the packing is solid spherical polymeric pellets of uniform diameter. An inert carrier gas carries a pulse of solvent through the packed bed. The pulse spreads in the column because of diffusion of the solvent into the polymer spheres and gas phase dispersion. A detector at the column exit measures the solvent gas concentration as a function of time. A schematic of the packed column is shown in Fig. 1.

Additional assumptions made:

1. The entire system is isothermal.
2. The polymer spheres all have the same radius.
3. The gas velocity is constant.
4. No pressure drop occurs over the column length.
5. The polymer phase diffusion coefficient is constant in the concentration range of the perturbation.
6. Axial dispersion in the gas phase can be well represented by an effective diffusion coefficient in the gas phase.
7. The thermodynamics of the gas–polymer interface can be described by a constant partition coefficient.
8. The carrier gas is insoluble in the polymer.
9. Surface adsorption by the solvent is described by a constant surface equilibrium constant.
10. The carrier gas cannot adsorb onto the polymer surface.
11. No chemical reactions occur.
12. The partial molar volume of the solvent in the polymer is constant.
13. Swelling of the polymer is insignificant.
14. The gas is well mixed in the radial direction.

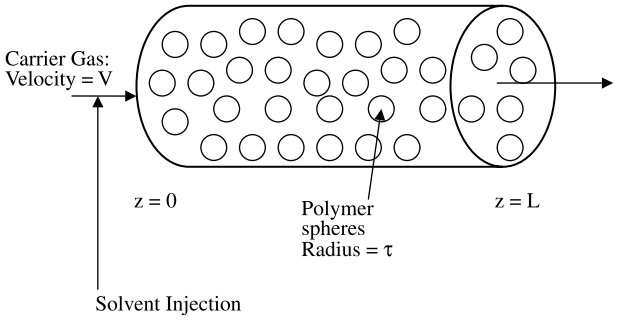

Fig. 1. Diagram of the packed column.

The model derivation that follows assumes a constant pressure/velocity in the column according to assumption 4. In a real packed column, there is a significant pressure drop. As is always the case in the analysis of PCIGC experiments, this pressure drop needs to be accounted for when determining the thermodynamic and diffusion coefficients. Details of this correction are presented in Section 3.3. Consider a single polymer sphere with a radius of τ. The governing equation and boundary conditions for diffusion in the polymer spheres are:

$$\frac{\partial \rho}{\partial t} = \frac{D_p}{r^2}\left(\frac{\partial}{\partial r}\left(r^2\frac{\partial \rho}{\partial r}\right)\right) \tag{1}$$

$$t = 0 \quad \rho = 0 \tag{2}$$

$$r = \tau \quad \rho = K_p C \tag{3}$$

$$r = 0 \quad \frac{\partial \rho}{\partial r} = 0 \tag{4}$$

For convenience, Eq. (1) can be non-dimensionalized. Definitions of the dimensionless variables can be found in the nomenclature section.

$$\frac{\partial(\rho' r')}{\partial t'} = \left[\frac{1}{\beta^2}\right]\frac{\partial^2(\rho' r')}{\partial r'^2} \tag{5}$$

In this equation, $\beta^2 = V\tau^2/LD_p$. This expression along with the dimensionless boundary conditions can be solved in the Laplace domain [14]:

$$Q = Y\left(\frac{e^{-\beta\sqrt{sr'}} - e^{\beta\sqrt{sr'}}}{e^{-\beta\sqrt{s}} - e^{\beta\sqrt{s}}}\right) \tag{6}$$

Here, Q is the Laplace variable for $\rho' r'$, Y is the Laplace variable for C'. The ultimate solution will also require the gradient of Q at the gas–polymer interface:

$$\left(\frac{\partial Q}{\partial r'}\right)_{r'=1} = Y\beta\sqrt{s}\coth(\beta\sqrt{s}) \tag{7}$$

Under the assumptions outlined above, the solvent species continuity equation and boundary conditions for the gas phase are:

$$\left(1 + \frac{3K_s(1-\chi)}{\chi\tau}\right)\frac{\partial C}{\partial t} + V\frac{\partial C}{\partial z} = D_g^{\text{eff}}\frac{\partial^2 C}{\partial z^2} - \frac{3(1-\chi)D_p}{\chi\tau}\frac{\partial \rho}{\partial r}\Big|_{r=\tau} \tag{8}$$

$$t = 0 \quad C = 0 \tag{9}$$

$$z = 0 \quad C = \delta(t)C_0 \tag{10}$$

$$z = \infty \quad C = 0 \tag{11}$$

Here, χ is the void fraction inside the column. Using the dimensionless variables defined in the nomenclature, Eq. (8) can be expressed in dimensionless form.

$$(1+\varepsilon)\frac{\partial C'}{\partial t'} + \frac{\partial C'}{\partial z'} = \gamma\frac{\partial^2 C'}{\partial z'^2} - \frac{3}{\alpha\beta^2}\left(\frac{\partial \rho' r'}{\partial r'}\Big|_{r'=1} - \rho' r'|_{r'=1}\right) \tag{12}$$

This equation combined with the polymer phase solution can be solved in the Laplace domain [14] to obtain the solvent concentration in the gas phase at the column exit:

$$Y = \exp\left\{\frac{1}{2\gamma} - \sqrt{\frac{1}{4\gamma^2} + \psi(s)}\right\} \tag{13}$$

$$\psi(s) = \frac{3\sqrt{s}\coth(\beta\sqrt{s})}{\alpha\beta\gamma} - \frac{3}{\alpha\beta^2\gamma} + \frac{(1+\varepsilon)s}{\gamma}$$

It is very difficult to analytically invert Eq. (13) back into the time domain, so solution of the model is accomplished by numerical inversion using a fast Fourier transform (FFT) algorithm.

3. Experimental section

3.1. Materials and equipment

A Varian 3700 gas chromatograph was used in these experiments. A schematic diagram is shown in Fig. 2.

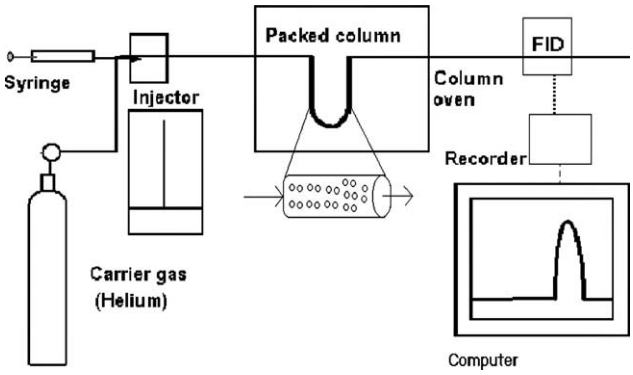

Fig. 2. Diagram of PCIGC apparatus.

The chromatograph was equipped with a flame ionization detector (FID), and helium was used as the carrier gas in all runs. The flow rate was regulated by the variation of the inlet pressure of the gas. The solvents were injected into the column at the injector port with a Hamilton 1 μL syringe. Twenty-five microliters of methane were injected into the column followed by an injection of the solvent. The signal from the FID was captured on a PC using LabView. The actual average velocity through the column was determined by measuring the retention time of the methane and the length of the column. Often, a gas flow meter is used in PCIGC experiments to estimate the vapor velocity. The tracer method used here is superior to the flow meter since the tracer incurs the pressure drop in the column, and responds the same as the injected solvents. This will prove an important part of the data analysis as described later.

Particles of metallocene-catalyzed, linear-low-density polyethylene (LLDPE) were mechanically sieved into batches of different diameters. Two sizes were selected for study. A Malvern MasterSizer was used to determine the size distributions. In each case relatively sharp distribution peaks were obtained with volume mean diameters of 235 and 360 μm. SEM pictures confirmed that these were good estimates. The characteristics of the polyethylene beads are shown in Table 1. The porosity of the polymer was determined using the mercury porisometry method. The bulk density, apparent density, and surface area were also determined. Crystallinity was calculated from the results of differential scanning calorimetry. The 235 μm beads were 43% crystalline and the 360 μm beads were 37% crystalline. The melt temperature of both samples was 124–125 °C. Scanning electron microscopy was used to scan the surface of the particles and appear in Figs. 3 and 4. The solvents used were *n*-pentane, isopentane, *n*-hexane, 1-hexene, and 1-octene. They were used as obtained from the Aldrich Company.

Table 1
Polymer bead characteristics

Diam. (μm)	$A_{surface}$ (m^2/g)	Porosity (%)	Bulk density (g/cm^3)	Apparent density (g/cm^3)	Crystallinity (%)	Melt T (°C)
235	0.346	14.6	0.770	0.901	43	125
360	0.165	10.1	0.907	1.009	37	124

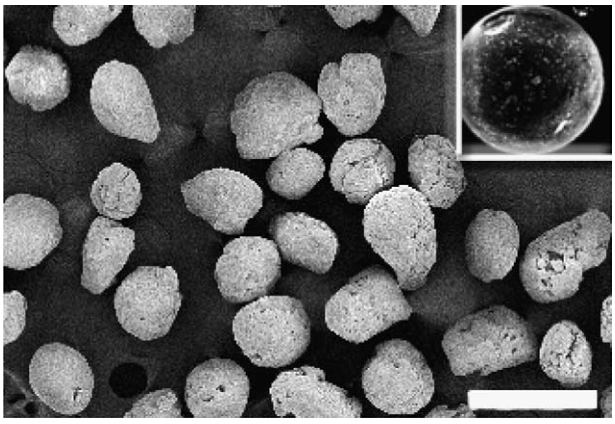

Fig. 3. SEM of 235 μm LLDPE beads. Insert, single particle. White bar = 500 μm.

Copper tubing with an outside diameter of 0.635 cm was bent into a 'U' shape, and washed with ethanol followed by chloroform to remove contaminants. The copper column was heated in the oven at a minimum of 50 °C for at least 4 h. The column was packed with approximately five grams (half a gram at a time) and vibrated to eliminate empty pockets. The ends of the copper tubing were plugged with glass wool to hold the packing in place. The characteristics of each column are listed in Table 2.

The column was conditioned to remove residual solvents from the beads. This was done by heating the column to a point just below the polymer's melting point and passing helium through the column. The temperatures for the column, injector, and detector were set.

3.2. Examples of raw data elution profiles

Figs. 5 and 6 show examples of the raw data elution profiles collected in the study. Scatter in the raw data varied significantly and depended upon the solvent and temperature. Peak shapes varied from relatively symmetrical (Fig. 5) to skewed (Fig. 6), depending on the diffusivity in the polymer. In addition, retention times varied significantly with solvent and

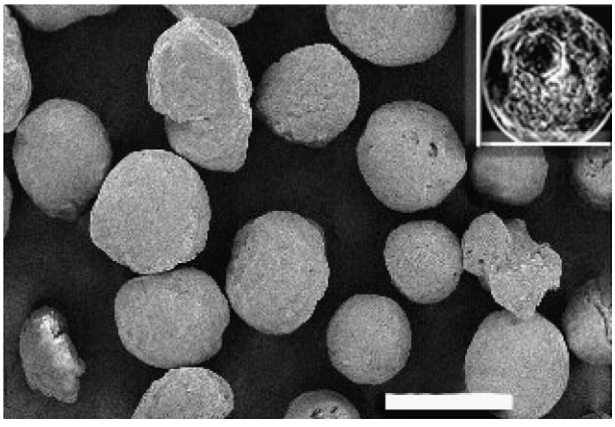

Fig. 4. SEM of 360 μm LLDPE beads. Insert, single particle. White bar = 500 μm.

Table 2
Column characteristics

Polymer bead size (μm)	Length (cm)	Outside diameter (cm)	Mass of polymer (g)	Void fraction (%)
235	46.4	0.635	5.392	29.0
360	45.7	0.635	5.286	29.5

temperature indicating strong sensitivity to the solvent partitioning.

3.3. Data analysis

Partition and diffusion coefficient measurements were made by the time domain fitting method. In this procedure, the dimensionless parameters (α and β) were optimized using a non-linear least squares Levenberg–Marquardt algorithm from the IMSL library such that the experimental elution profile best matched the model profile from Eq. (13). The diffusion and partition coefficients from the first and second moments were used as initial guesses for the regression algorithm. In this analysis, the ε was set to zero and eliminated from the fitting procedure since introducing it gave no better correlation of the data. This indicated that surface adsorption was a negligible retention mechanism compared to bulk absorption.

Typically, retention volumes or moments are used to estimate the partition coefficient and diffusivity. It is well understood that such values are inherently incorrect due to the velocity change through the packed column due to the gas phase pressure drop. Values are typically corrected using a *j*-factor [15], which accounts for the velocity effects. In this work, a time domain fitting procedure was used. Actual chromatograms obtained under conditions of significant pressure drop were compared to model chromatograms that were generated assuming no pressure drop. To correct for this, the inert methane chromatograms were first fit to the model. Since methane did not significantly absorb in the polymer or adsorb on the surface, it was assumed that all peak spreading was due to axial dispersion and the methane retention time represented the average carrier gas velocity. The velocity and effective vapor phase diffusivity (γ parameter) from the methane fits were then used in the model while regressing

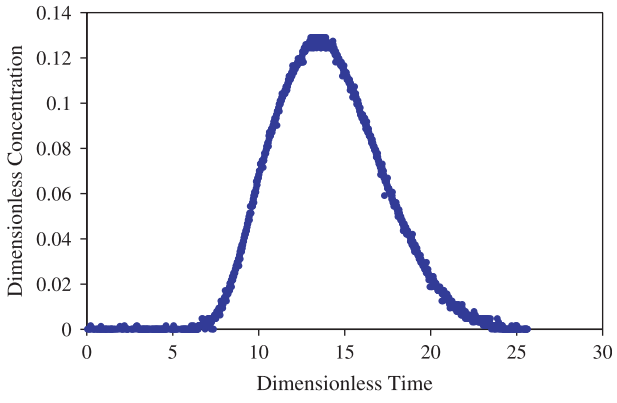

Fig. 5. Raw data elution profile for *n*-hexane-360 μm beads at 80 °C.

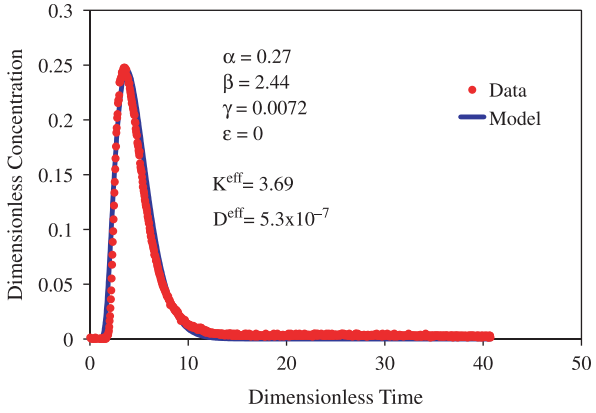

Fig. 6. Model correlation of elution profile for isopentane-235 μm beads at 60 °C.

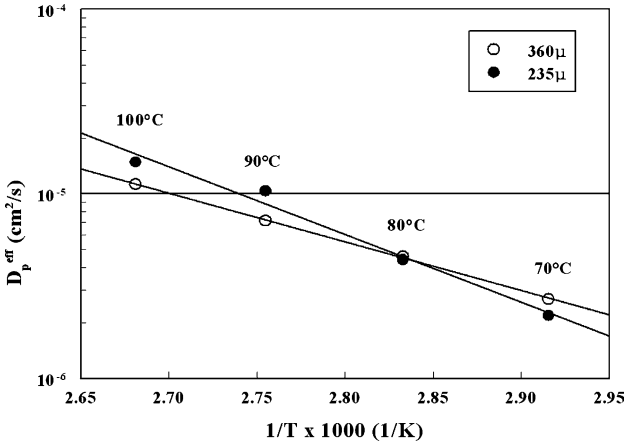

Fig. 8. Diffusivity of *n*-pentane in LLDPE beads.

the solvent experimental data. This approach is less empirical than the *j*-factor technique and provides more insight into the relative contributions of axial dispersion versus polymer diffusion. An example of the model fit to the methane tracer elution profile is shown in Fig. 7. In many cases, γ made a very significant contribution to the spread of the elution profile indicating that diffusion resistance in the polymer was a weak spreading mechanism compared to axial dispersion.

Regression for α and β yielded partition and diffusion coefficients. However, these coefficients were not true values due to the crystal content and porous nature of the LLDPE pellets. It is typically assumed that no solvent can absorb into the crystalline regions of the polymer, thus the solvent molecules must diffuse around them in a tortuous path. As a result, the crystals tend to lower the effective diffusion and partition coefficients. Also, the pores in the pellets tend to give effectively larger diffusion coefficients since gas phase diffusion is much faster than that in the polymer. These pores also tend to effectively reduce the partition coefficient since the sample's solvent capacitance is reduced compared to the same volume of solid (non-porous) particle. Although the pores and crystals complicate measuring the true mutual binary diffusion coefficient and partition coefficient, the goal of this study is to determine the effective partition (K^{eff}) and diffusion (D^{eff}) coefficients since it is these effective coefficients that are needed in calculations for devolatilization of such particles.

Calculation of the effective partition coefficient from α requires the column void fraction, χ, as shown in Table 2. In all cases, the model provided a good correlation of the experimental elution profiles. An example of the correlation is given Fig. 6.

4. Results

The effective diffusion coefficients for the various systems are shown in Figs. 8–10. As expected all the diffusion coefficients increased as the temperature increased, that is as the free volume in the pellets increased. There are a number of complications when it comes to analyzing the variation of the diffusivity between the two samples. While the smaller particles have higher porosity, they also have a higher crystallinity. These two morphological effects tend to cancel each other, giving similar effective diffusivities for both particle sizes.

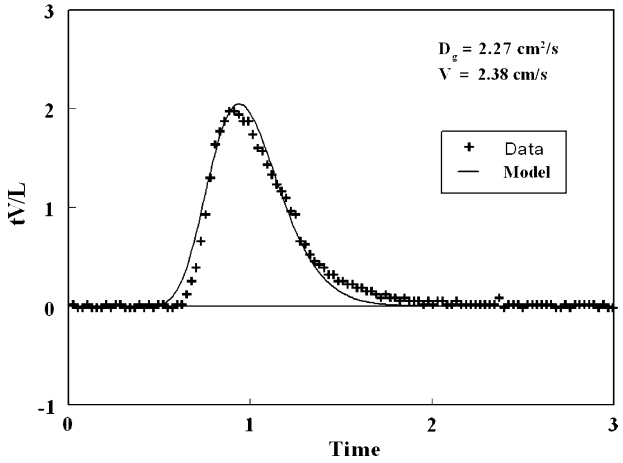

Fig. 7. Methane peak.

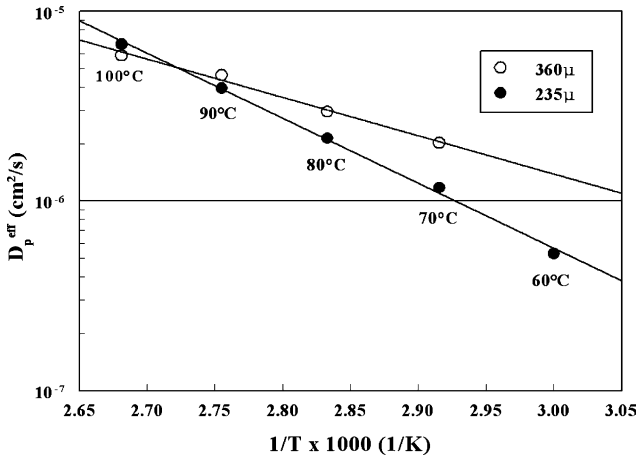

Fig. 9. Diffusivity of isopentane in LLDPE beads.

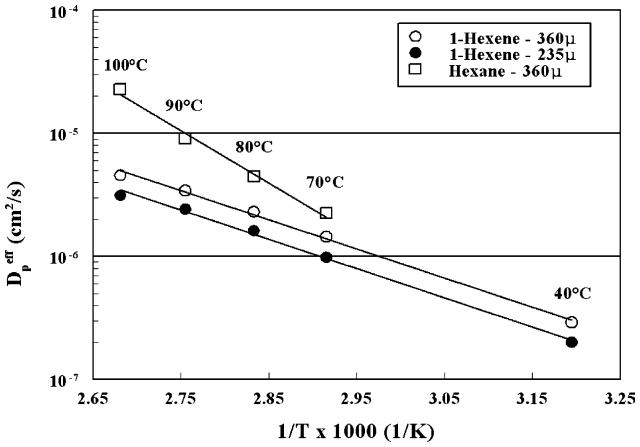

Fig. 10. Diffusivity of *n*-hexane and 1-hexene in LLDPE beads.

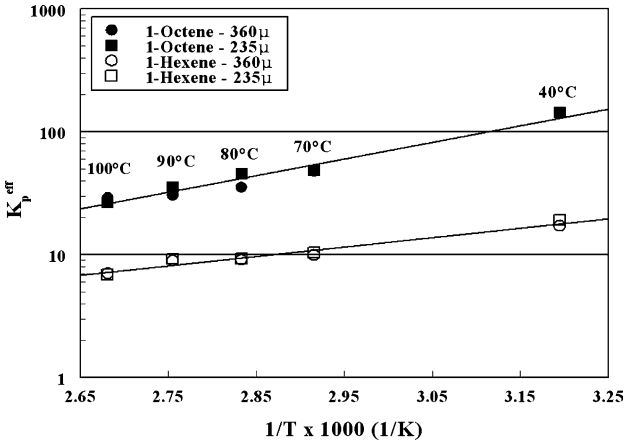

Fig. 11. Effect of LLDPE bead size on sorption.

All effective diffusion coefficients were well correlated by an Arrhenius type expression:

$$D^{\text{eff}} = D_0 \exp\left(\frac{-E^{\text{eff}}}{RT}\right) \tag{14}$$

Here, D_0 is a temperature independent pre-exponential factor, and E^{eff} is the effective activation energy of diffusion. The Arrhenius coefficients are listed in Table 3.

The model (Eq. (13)) indicates that for a short, packed column the spreading of the elution peak increases with an increase in the distribution coefficient K_p. Consequently, for the higher boiling solvents, which have high solubilities and large values of K_p, it is difficult to determine the additional spreading of the elution curve due to the diffusion of the solvent in and out of the polymer phase. From the fitting of the experimental elution curves with the model, accurate K_p and D_p results were obtained for *n*-pentane, isopentane, 1 hexane, and *n*-hexane. However, for 1-octene, which has a much higher solubility (large K_p), the axial dispersion due to mixing in the gas phase masked the elution peak spreading due to diffusion in the polymer phase. Consequently, reliable values of D_p could not be obtained for 1-octene.

Measurement of the partition coefficient does not depend on axial dispersion effects, and partition data were able to be obtained for all systems studied. From the partition coefficients for the two different particle sizes shown in Fig. 11, it is clear that surface adsorption is an insignificant retention mechanism compared to bulk sorption. No difference in partitioning was obtained using particles of varying surface area to volume ratios. This was also verified by including the ε parameter in the data analysis. There was no improvement in the fits with ε included, indicating insignificant surface adsorption. As a result of this, no surface adsorption information could be obtained from the data. All partition data gave the usual trend that the larger molecules had the higher solubilities as shown in Fig. 12. Additionally, all solvent partition coefficients decreased with increasing temperature as is usually seen.

All effective partition coefficient data fit well to an Arrhenius type expression:

$$K^{\text{eff}} = K_0 \exp\left(\frac{-\Delta H^{\text{eff}}}{RT}\right) \tag{15}$$

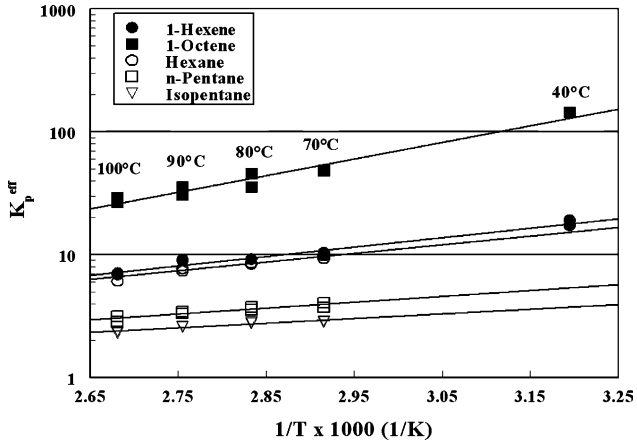

Fig. 12. Solubility of solvents in LLDPE beads.

Table 3
Arrhenius parameters for D^{eff}

Solvent	Bead diameter (μm)	D_0 (cm²/s)	$-E^{\text{eff}}/R$
n-Pentane	235	1.14×10^5	8455
	360	125	6053
Isopentane	235	3315	7456
	360	1.1.616	4660
n-Hexane	360	5.075×10^6	9785
1-Hexene	235	8.114	5473
	360	11.09	5454

Table 4
Arrhenius parameters for K^{eff}

Solvent	K_0	$\Delta H^{\text{eff}}/R$
n-Pentane	0.1109	1227
Isopentane	0.2313	872
n-Hexane	0.0845	1627
1-Hexene	0.0647	1758
1-Octene	0.00614	3115

Here, K_0 is a temperature independent pre-exponential factor, and is the effective heat of absorption. The fitted pre-exponential parameters and effective heats of absorption are given in Table 4.

5. Summary and conclusions

An experimental technique has been developed to measure effective diffusion and partition coefficients in binary polymer–solvent systems. The technique is a variation of packed column inverse gas chromatography in which the stationary phase is small polymer pellets. The usefulness of the technique is that effective partition and diffusion data can be obtained on the actual polymer pellets from a reactor that need to be devolatilized of residual monomer and solvents. Since the pellets are not melted or dissolved, the morphology and structure are not changed in any way during the experiments.

The LLDPE was obtained in two different particle diameter batches, 235 and 360 μm. Effective partition coefficients were collected at infinite dilution for all systems and the data correlated well with Arrhenius temperature dependence. The partition coefficients exhibited no dependence on the particle size of the beads. This indicated that, at least in the size range used in this study, surface adsorption is of no significance. Effective diffusion coefficients could not be obtained for the 1-octene because axial dispersion was the dominant peak spreading mechanism. For the other solvents effective diffusion data were also correlated with an Arrhenius temperature dependence. In general, the diffusion coefficients also appeared to have little dependence on the particle size.

References

[1] Danner RP, Tihminlioglu F, Surana RK, Duda JL. Fluid Phase Equilib 1998;148:171.
[2] Galassi S, Audisio G. Die Makromol Chem 1974;175:2975.
[3] Glass AS, Larsen JW. Macromolecules 1993;26:6354.
[4] Gray DG, Guillet JE. Macromolecules 1972;5:316.
[5] Guillet JE, Galin M. J Polym Sci, Part C: Polym Lett 1973;11:233.
[6] Hadj Romdhane I. Polymer–solvent diffusion and equilibrium parameters by inverse gas–liquid chromatography. Thesis in chemical engineering; 1994.
[7] Joffrion LL, Glover CJ. Macromolecules 1986;19:1710.
[8] Macris A. Measurement of diffusion and thermodynamic interactions in polymer–solvent systems using capillary column inverse gas chromatography. Thesis in chemical engineering; 1979.
[9] Pawlisch CA, Laurence RL, Macris A. Macromolecules 1988;20:1564.
[10] Smidsrod O, Guillet JE. Macromolecules 1968;2:272.
[11] Surana RK, Danner RP, Tihminlioglu F, Duda JL. J Polym Sci, Part B: Polym Phys 1997;35:1233.
[12] Arnould DD. Capillary column inverse gas chromatography (CCIGC) for the study of diffusion in polymer solvent systems. Thesis in chemical engineering; 1989.
[13] Braun JM, Guillet JE. Macromolecules 1976;9:340.
[14] Davis PK. Experimental and theoretical aspects of studying thermodynamics and mass transport in polymer–solvent systems. Thesis in chemical engineering; 2003.
[15] Condor JR, Young CL. Physical measurement by gas chromatography. New York: Wiley-Interscience Publication; 1979 [chapter 2].